

Bioerosion on the small scale – examples from the tropical and subtropical littoral

Miklós KÁZMÉR¹ & Danko TABOROŠI²

(with 96 figures and 1 table)

The purpose of this paper is to provide a practical guide assisting field workers in identification and interpretation of bioerosional textures created in limestone and other substrates by intertidal organisms. We provide examples of living, dead, and subfossil bioerosional agents and their corresponding traces. The discussion follows taxonomic order of bioerosional agents, rather than morphologic classification of their effects on the rock substrate. Traces left by sponges, molluscs (chiton *Acanthopleura*, limpets and various gastropods, bivalves *Lithophaga* and *Tridacna*, wood-boring bivalves), worms, echinoid *Echinometra*, and other taxa are illustrated. Features created by a distinct group of organisms but exhibiting excellent, average, and poor levels of preservation are displayed alongside each other to help identification under suboptimal conditions. We also show composite textures resulting from successive or coeval overlapping traces, and offer examples of pseudo-bioerosional features reminiscent of organism traces but created by physical processes.

Introduction	38
Bioeroders and their traces	38
Microorganisms	38
Sponges	41
Chitons	44
Homing scars	46
Grazing traces	47
Gastropods	52
Limpets	52
Littorinid gastropods	55
Drilling gastropods	58
Bivalves	59
Lithophaga	59
Tridacna	66
Wood-boring bivalves	67
Worms	68
Sea urchins	68
Echinometra	68
Fossil echinoid burrows	76
Crabs	80
Grapsid crabs	80
Competition and/or succession of bioeroders	81
Pseudo-bioerosion	88
Acknowledgements	92
References	92

¹ Department of Palaeontology, Eötvös University, H-1117 Budapest, Pázmány Péter sétány 1/c, Hungary.
E-mail: mkazmer@gmail.com

² Water and Environmental Research Institute of the Western Pacific, University of Guam, Mangilao, Guam 9692, USA. Email: taborosi@gmail.com

Introduction

Bioerosion has been well studied on microscopic scale (microbioerosion; see, for example, GLAUB et al., 2007) and on the macro-scale (coastal landforms; see, for example, SPENCER and VILES, 2002). Here we provide a rich selection of examples of bioerosion observed at meso-scales: traces of individual organisms forming marine notches and other bioerosional features in the intertidal zone. The purpose of the paper is to provide a practical guide assisting field workers in identification and interpretation of bioerosional textures created in limestone and other substrates by intertidal organisms. We provide examples of living, dead, and subfossil bioerosional agents and their corresponding traces. Features created by a distinct group of organisms but exhibiting excellent, average, and poor levels of preservation are displayed alongside each other to help identification under suboptimal conditions.

The discussion follows taxonomic order of bioerosional agents, rather than morphologic classification of their effects on the rock substrate. Traces left by sponges, molluscs (chiton *Acanthopleura*, limpets and various gastropods, bivalves *Lithophaga* and *Tridacna*), echinoid *Echinometra*, and other taxa are illustrated. Various states of preservation, from excellent to barely recognizable, are presented. In addition, we show composite textures resulting from successive or coeval overlapping traces produced by different taxa, and several examples of features reminiscent of bioerosion but created by physical processes. Photographs are described in detail. Examples are taken from the carbonate coasts of the Mediterranean, Japan, Thailand, various Pacific Islands, and several other locations.

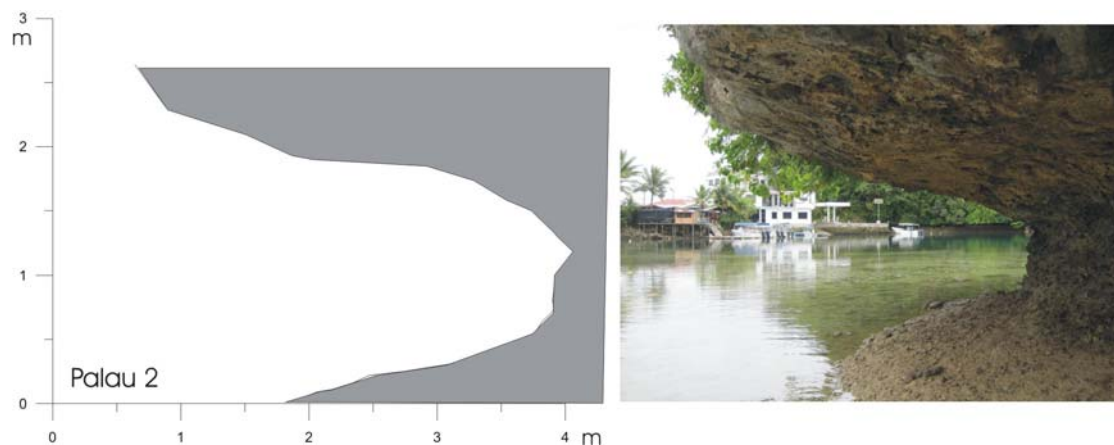


Fig. 1. Marine notch along the Koror-Malakal dam, Palau. Cross section surveyed according to KÁZMÉR & TABOROŠI (2012). The roof, back wall and floor of the notch bear a rich variety of bioerosion traces. Photo Kázmér #101.9767.

Bioeroders and their traces

Microorganisms

Microorganisms, mostly cyanobacteria, but also bacteria, algae, and marine fungi, are all known to attack limestone substrates and produce identifiable scars. Various traces created by

individual microbes are on microscopic scale and are thus beyond the scope of this paper, but there are several compound textures that are commonly observed on medium (centimetre to decimetre) scales. They are observed only in places where they are not quickly overprinted by eroding activity of larger organisms. In temperate regions, microbial activity is best recorded as dark belts along upper intertidal zone and blotches in areas of wave splash accumulation. In tropical regions, microbial effects on coastal rocks are most evident in the form of ubiquitous „phytokarst” – highly irregular and extraordinarily jagged type of karren that develops in eogenetic limestones attacked by boring cyanobacteria (e.g., Jones, 1989).

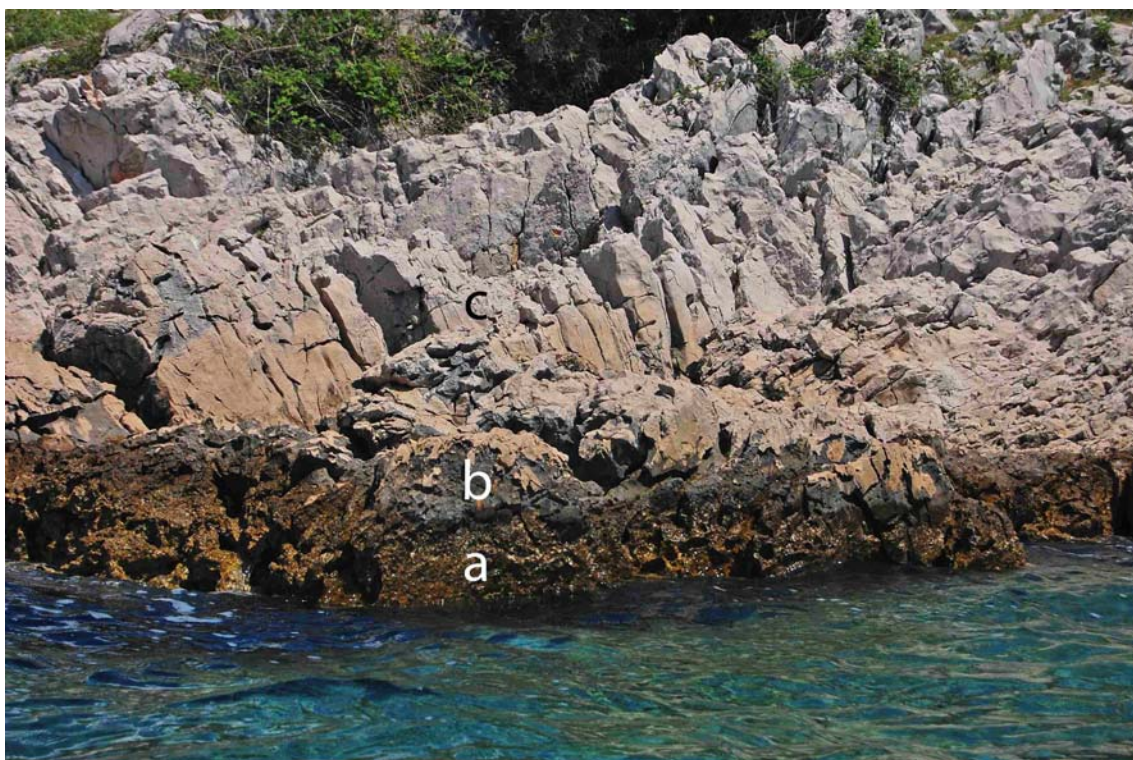


Fig. 2. Color belts of microbial origin observed in coastal rocks along the Adriatic Sea coastline. **a.** Brownish (intertidal) and **b.** grey (lower supratidal) belts marking the transition between permanently submerged rock and **c.** light colored bedrock beyond the regular influence of seawater. Kraljevica, Croatia. Photo: Taboroši #DSC_9591.



Fig. 3. Grottesquely sculpted “phytokarst” in diagenetically immature coral limestone. Guam. Photo: Taboroši #DSC_1121 .



Fig. 4. Closeup of dark colored rock surface in the lower supratidal zone along the Adriatic Sea coastline. Note that the original light-colored and relatively smooth rock surface is being progressively corroded and replaced by dark-colored pitted surface due to microbial activity. Bottle cap for scale. Kraljevica, Croatia. Photo: Taboroši #DSC_9646 .



Fig. 5. Highly irregularly eroded supratidal limestone surface is a compound result of dissolution, salt weathering, and erosive action of endolithic cyanobacteria and possibly other microbes. Lens cap 52 mm diameter. Boracay, Philippines. Photo: Taboroši #DSC_1076 .

Sponges

Certain sponges, notably *Cliona* spp., are known to penetrate calcareous substrates (rock and shells) and produce interconnected networks of voids whose overall morphology is reminiscent of sponge's own anatomy (Ekdale et al., 1984). They appear as numerous small apertures in rock surfaces and reveal complex internal networks if broken by a hammer. While the sponge is alive, brightly colored sponge tissue can be seen emerging from the openings in the rock surface or is observed thoroughly covering the rock surface (and concealing the openings).



Fig. 6. *Cliona celata* boring sponge. The chambered portion within the rock is overgrown by a bright yellow tissue, effectively making the sponge look like it is coating the rock rather than boring into it. Saint-Quay-Portrieux, Bretagne, France. Photo: Matthieu Sontag http://en.wikipedia.org/wiki/File:Cliona_celeta.JPG. Licence CC-BY-SA

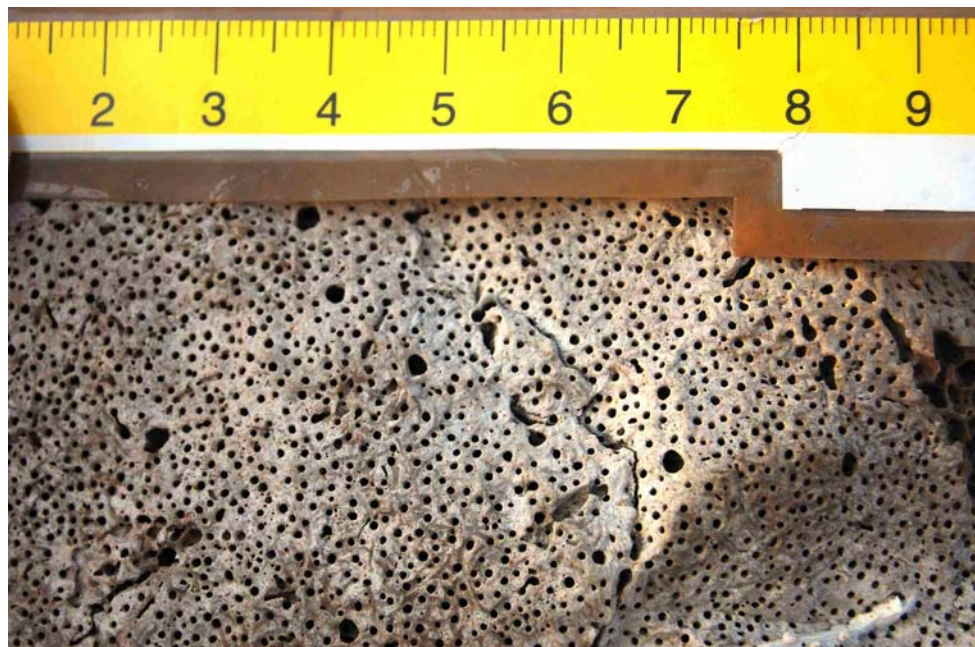


Fig. 7. Numerous small-diameter boreholes are a typical surface expression of endolithic activity by a boring sponge. The surface has not been eroded after sponge's death: these are the original openings into interior chambers that hosted the bulk of the animal's body. Scale in centimetres. Kraljevica, Croatia. Photo: Taboroši #DSC_9766

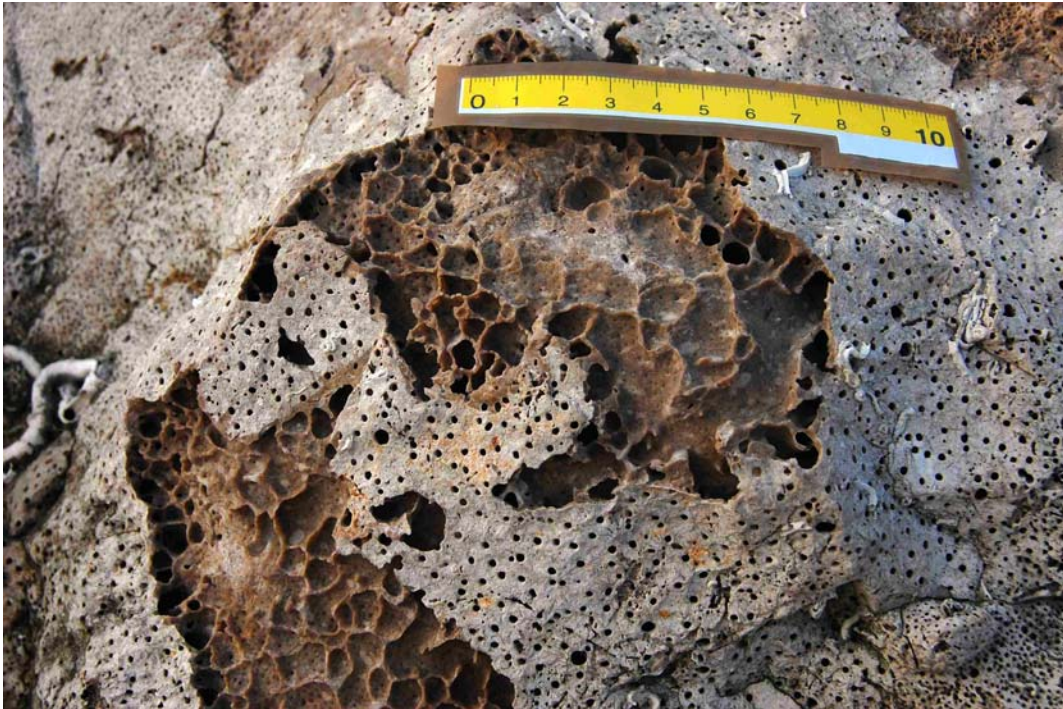


Fig. 8. Honeycomb-like galleries that used to host the main body of a boring sponge have been revealed by natural breakage of the surface rock layer. Areas where the surface has not been broken exhibit only small diameter openings originally used by the sponge to interface with the outside environment. Scale in centimetre. Kraljevica, Croatia. Photo: Taboroši #DSC_9761 .

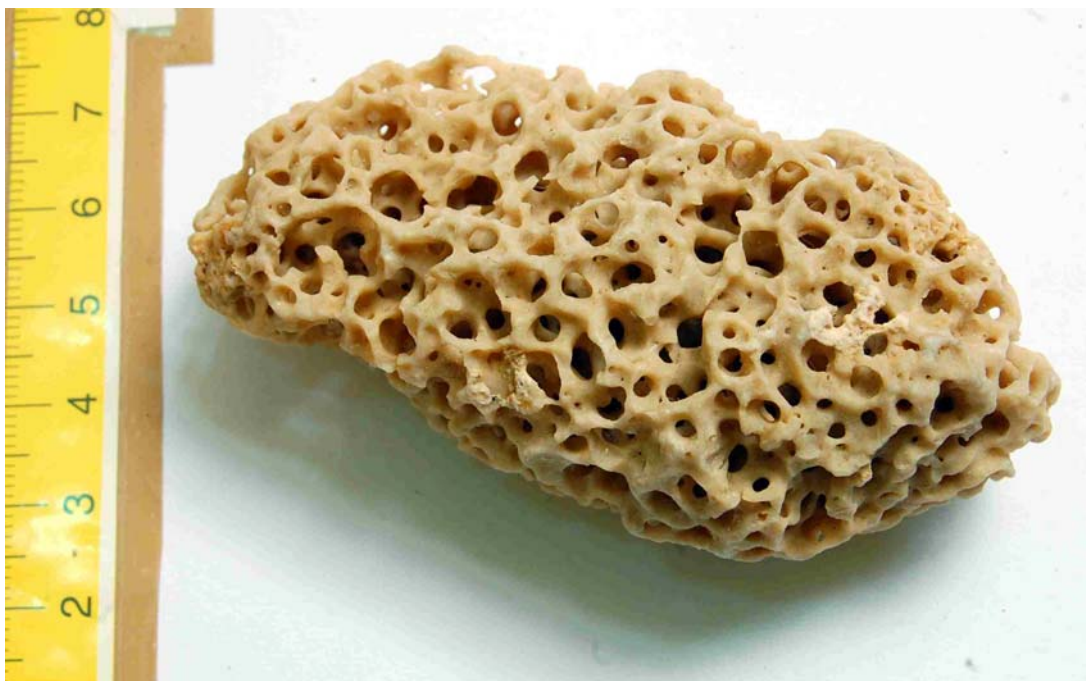


Fig. 9. DSC_9880. Hand specimen thought to have been a rock permeated by a boring sponge and then smoothed by wave action in a sandy beach environment. Scale in centimetres. Socotra, Yemen. Photo: Taboroši #DSC_9880 .

Chitons

Chitons are the some of the most obvious eroders of the intertidal zone: their 8-plated shell and a colourful margin of soft tissue make them conspicuous in many sites. They are armed with a radula of extremely hard magnetite-capped teeth that allow them to easily remove layers of calcium carbonate and other substrates. Their rasp marks are usually meandering or straight sets of parallel grooves engraved into substrate. They also produce pronounced homing scars – larger pits that accommodate an individual animal's body size and represent its long term residence.



Fig. 10. This feeding chiton (*Acanthopleura*) produced audible rasping when observed and photographed. . Coin 24 mm diameter. Palau. Photo Kázmér # 101.9791.

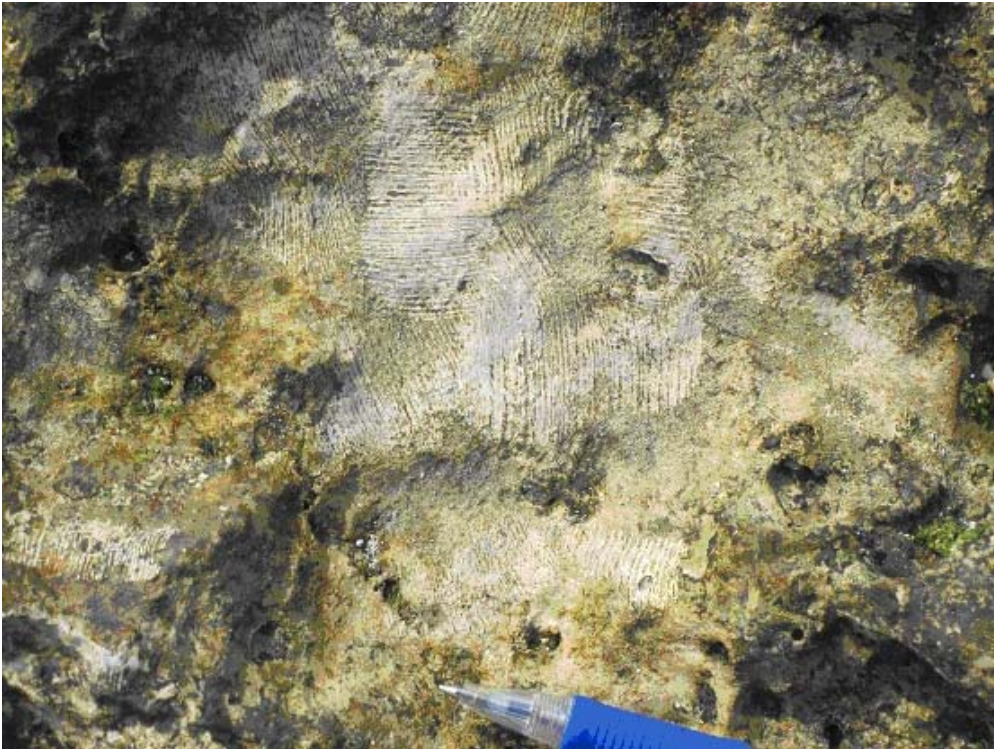


Fig. 11. Fresh grazing traces of a chiton. Green epilithic algae have been rasped by the radula together with the uppermost layer of rock inhabited by endolithic algae. Pen 12 mm diameter. Okinawa, Japan. Photo: Kázmér: #101.8491



Fig. 12. White chiton pellets scattered over a turf of green algae. The white colour is due to 96% CaCO₃ content. Image width 16 cm. Okinawa, Japan. Photo Kázmér #101.8732.

Homing scars

Fig. 13. Chiton *Acanthopleura* inside its homing scar, carved in a steep notch floor. Coin 21 mm diameter. Palau. Photo: Kázmér # 101.9780.



Fig. 14. Chiton *Acanthopleura* in a self-made (?) homing scar. The hole has diameter ca. 5 cm, making it similar to a sea urchin borehole, but distinguished by its irregular walls. Note white fecal pellets, 96 wt% calcium carbonate (RASMUSSEN & FRANKENBERG, 1990). Malakal, Palau (Photo: Kázmér #101.9789)



Fig. 15. Chiton *Acanthopleura* in a homing scar during low tide. White pellets contain 96 wt% CaCO_3 . Coin 21 mm diameter. Malakal, Palau (Photo: Kázmér #101.9796)

Grazing traces



Fig. 16. Composite pattern of long-term chiton grazing activity. Deep holes are probably homing scars of young animals. They may be confused with sea urchin boreholes but are less regular shaped. Pen 12 mm diameter. Railay, Thailand. Photo: Kázmér #102.0602



Fig. 17. Texture formed in the floor of a marine notch exposed to long-term chiton grazing. Deep holes may be former homing scars, overprinted and resculpted by subsequent grazing. Pen 12 mm diameter. Railay, Thailand. Photo: Kázmér #102.0777.

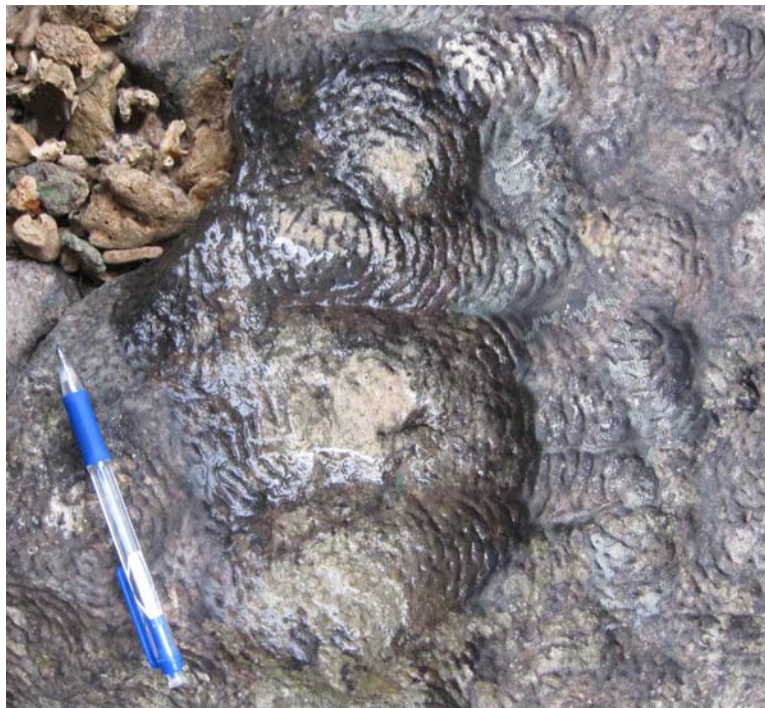


Fig. 18. Arcuate pattern on the floor of a marine notch exposed to long-term chiton grazing. Pen 12 mm diameter. Railay, Thailand. Photo: Kázmér #102.0778.



Fig. 19. Repetitive pattern on the floor of a marine notch exposed to long-term chiton grazing. Grazing has been inactive at least since the barnacle (off center) settled. Pen 12 mm diameter. Railay, Thailand. Photo: Kázmér #102.0901.



Fig. 20. Long inactive traces of chiton grazing seen on the surface of a slightly eroded boulder. Okinawa. Photo: Kázmér #101.8711.

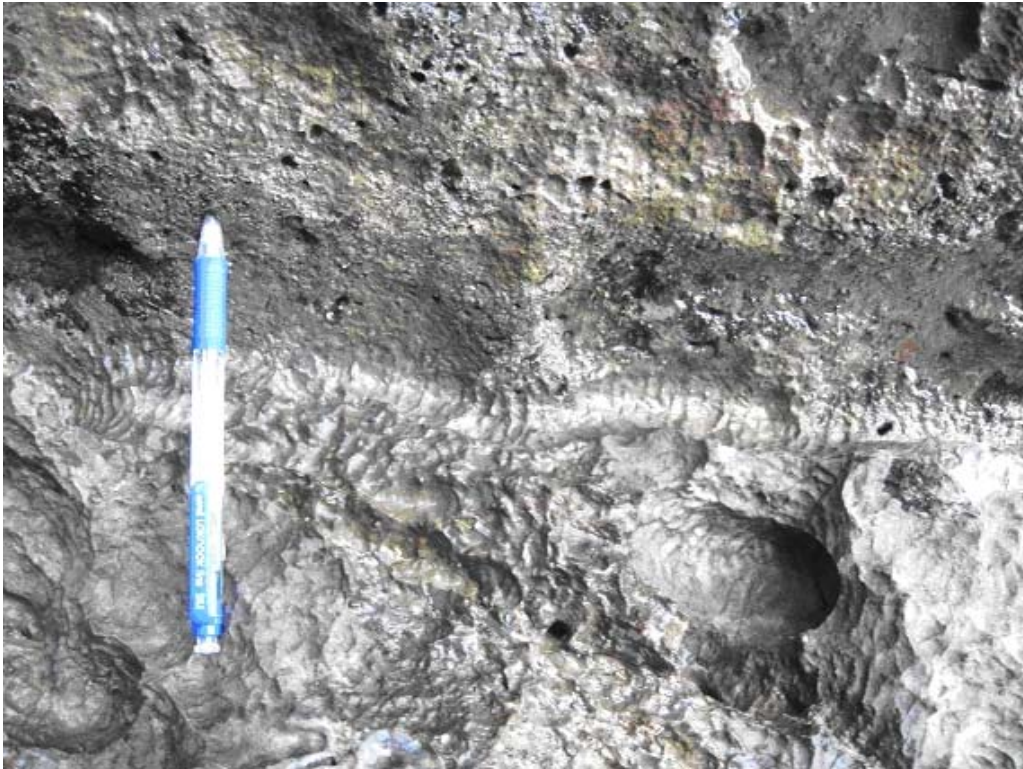


Fig. 21. Horizontal groove produced by chitons along the vertex of a recently uplifted notch. Chiton-grazed zones can be seen above and below, as well. Pen 12 mm diameter. Railay, Thailand. Photo: Kázmér #102.0592



Fig. 22. Chiton grazing traces on rock surface and a breached oyster shell. Coin 24 mm diameter. Malakal, Palau. Photo: Kázmér #101.9797



Fig. 23. Chiton grazing traces on rock and an oyster shell. Holes in the shell were made by shell thinning and wearing out caused by chiton grazing. Coin 24 mm diameter. Malakal, Palau. Photo: Kázmér #101.9787



Fig. 24. Chiton grazing traces on rock and surfaces of oyster shells. Malakal, Palau. Photo: Kázmér #101.0891

Gastropods

Limpets

Limpets are gastropods with a conical, uncoiled shell and a broad foot. They are known for the way they tightly cling to rock and are ubiquitous in intertidal and lower supratidal zones. They possess radula with silica-containing teeth used to scrape algae off and from within rock substrate. Limpet activity on rock surfaces produces rasping marks and homing scars that often correspond exactly to the size and shape of an individual's shell.



Fig. 25. Limpet hiding in its homing scar during low tide. Note that scar shape closely follows shell outline at rib terminations. Shell ca. 2.5 cm long. Okinawa. Photo: Kázmér #101.8730.



Fig. 26. Limpet hiding in a homing scar. Note that scar shape closely follows shell outline, indicating that it was created by this very individual over the course of its growth. Shell 24 mm long. Palau. Photo: Glumac #2374.



Fig. 27. Closeup of a limpet in its homing scar. Note the shadow-accentuated difference in relief between the scar and surrounding rock. Shell 3 cm long. Guam. Photo: Taboroši #DSC_3770 .



Fig. 28. Algae-coated limpet hiding in a homing scar. Note that the shell is smaller than the scar: probably the animal occupied a previously-existing homing scar of a larger animal. Shell 7 mm long. Okinawa. Photo: Kázmér #101.8279

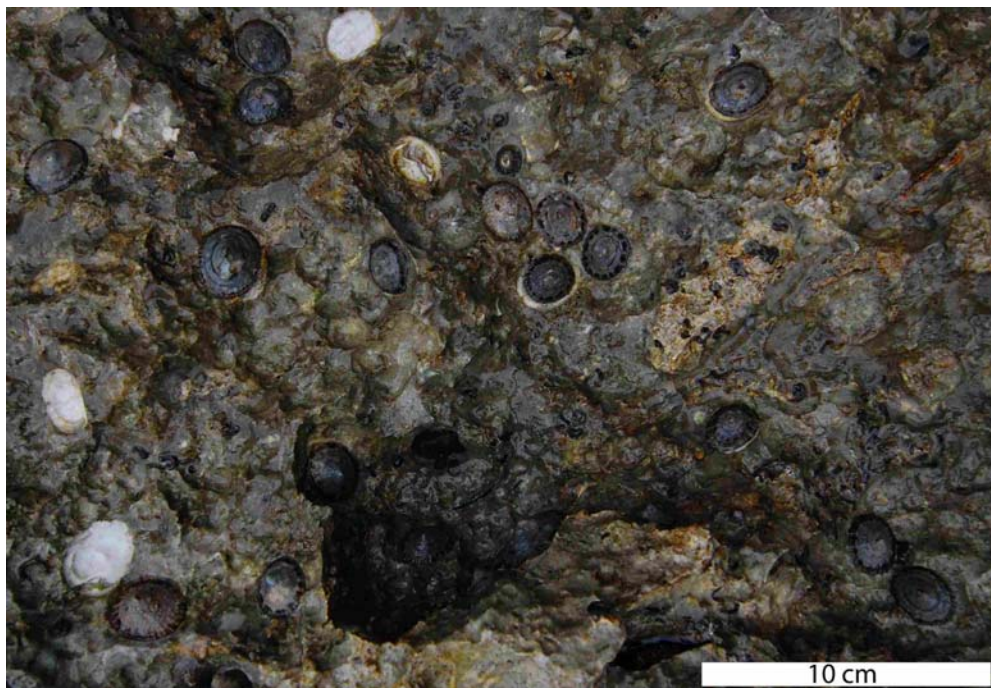


Fig. 29. Group of limpets clinging to wave-splashed rock in intertidal zone. Dark circles are shells of living limpets. Light circles are scars left behind in places where limpets have been naturally removed. Color contrast is due to the lack of microbial biofilm in scarred areas. Also note the contrast between smooth surfaces of limpet scars and the rough appearance of surrounding rock. Guam. Photo: Taboroši #DSC_1209 .



Fig. 30. Various limpets grazing or hiding in homing scars. Image ca. 40 cm wide. Okinawa. Photo: Kázmér #101.8273

Littorinid gastropods

A range of other gastropods, specifically littorinid snails but other genera as well, are known to inhabit rocky shorelines around the world and specialize in scraping biofilms and turf algae off exposed surfaces. Some of them appear to be capable of scratching the rock with their radulas and consuming endolithic organisms as well. Though they do not leave bioerosional traces visible to the naked eye, they do contribute to the overall bioerosional process and lowering of the bedrock surface. In the field, evidence for destruction of the bedrock can be seen in the form of CaCO_3 -rich fecal pellets left behind by grazing animals.



Fig. 31. A littorinid gastropod grazing the algal coating of a carbonate rock. Though there are no grazing traces observable by naked eye, the white-coloured CaCO_3 -rich excrement indicates that the surface layer of limestone has been scraped off while grazing. Scale in centimetres. Palau. Photo: Glumac #P7040135



Fig. 32. A group of littorinid snails grazing on highly eroded upper intertidal rock. Guam. Photo: Taboroši #DSC_0569 .



Fig. 33. A group of littorinid snails feeding on epilithic algae. Puerto Rico. Photo: Taboroši #DSC_1692 .



Fig. 34. Small gastropods grazing on the algal coating on the floor of an intertidal pool. Sand grains pushed away during their progress mark the paths of individual animals. They leave no appreciable grazing marks on the rock surface as they pass. Pen 12 mm diameter. Railay, Thailand. Photo: Kázmér #102.0582

Drilling gastropods

An interesting type of bioerosional trace is produced by predatory gastropods that feed on bivalves. They produce characteristic drill holes commonly observed in sea shells on sandy beaches. Drill holes are not observed in rock substrates because their purpose is to provide access to the soft tissue of living prey.



Fig. 35. Bivalve shells with drill holes made by predatory gastropod at the time organisms were alive. Hokkaido, Japan. Photo: Taboroši #DSC_0082.

Bivalves

Lithophaga

Unlike gastropods, which are typically motile surface scrapers, bivalves include powerful bioeroders that are largely sessile and physically and chemically bore into rocks as means of protection from predators. They enlarge bored voids as they grow and gradually reduce the overall volume of host rock from within.

Best known rock-boring bivalves belong to *Lithophaga* genus, which create deep club-shaped cavities that accommodate the shell and increase in diameter with the growth of the organism. The boreholes have dumbbell-shaped openings at the rock surface, the shape corresponding to the organism's inhalant and exhalant siphons. Once the top layers of the rock have been eroded, the original dumbbell form is lost and the opening assumes a more circular shape. With further erosion, only the deepest ends of boreholes become visible as conical pits before they are completely destroyed.



Fig. 36. Living *Lithophaga* boring bivalves. Soft parts are visible through dumbbell-shaped openings corresponding to the animals' double siphon morphology. A light-coloured, calcareous lining can be seen on the walls of the hole in the center of the image. Dumbbell-shaped opening 14 mm long. Railay, Thailand. Photo: Kázmér #101.0881



Fig. 37. Living *Lithophaga* boring bivalves. Soft parts visible through dumbbell-shaped openings. There is no calcareous lining apparent on the holes' walls. Coin 20 mm diameter. Okinawa. Photo: Kázmér #101.8440



Fig. 38. Tightly packed group of dumbbell-shaped openings created by living *Lithophaga* boring bivalves. The hole in the upper right corner has a light-coloured calcareous lining. Picture 60 mm wide. Railay, Thailand. Photo: Kázmér #101.0882



Fig. 39. Clusters of *Lithophaga* dumbbell-shaped surface expressions of living individuals with retracted double siphons. Pen 12 mm diameter. Railay, Thailand. Photo: Kázmér #102.0570



Fig. 40. Living *Lithophaga* boring bivalves with clearly visible white linings on borehole walls. The function of the linings is unclear but may be protection against development of biofilms and algal overgrowths. Pen 12 mm diameter. Railay, Thailand. Photo: Kázmér #102.0589



Fig. 41. Eroded *Lithophaga* boreholes exhibiting circular, ellipsoidal, and conical cross-sections. Pen 12 mm diameter. Railay, Thailand. Photo: Kázmér #102.0811



Fig. 42. There are at least two generations of *Lithophaga* boreholes here, preserved intact (dumbbell shape) or eroded to various depth (rounded shape). Round holes 10-12 mm diameter. Railay, Thailand. Photo: Kázmér #102.0571



Fig. 43. A series of similarly-shaped *Lithophaga* boreholes, exposed to about half of their original depth. Both the smaller and younger dumbbell-shaped superficial openings and partly eroded, adult-sized cross-sections of an older generation holes exposed at depth are visible. Pen 12 mm diameter. Railay, Thailand. Photo: Kázmér #102.0571



Fig. 44. Texture reminiscent of 'Swiss cheese' developed on the surface of Permian limestone thoroughly bored by *Lithophaga* during the last interglacial highstand. Following the attack by boring bivalves, the surface has been exposed to additional bioerosion (incomplete boreholes) and wave erosion (smooth ridges). Pen 12 mm diameter. James Bond Island, Phang Nga, Thailand. Photo: Kázmér #101.6817

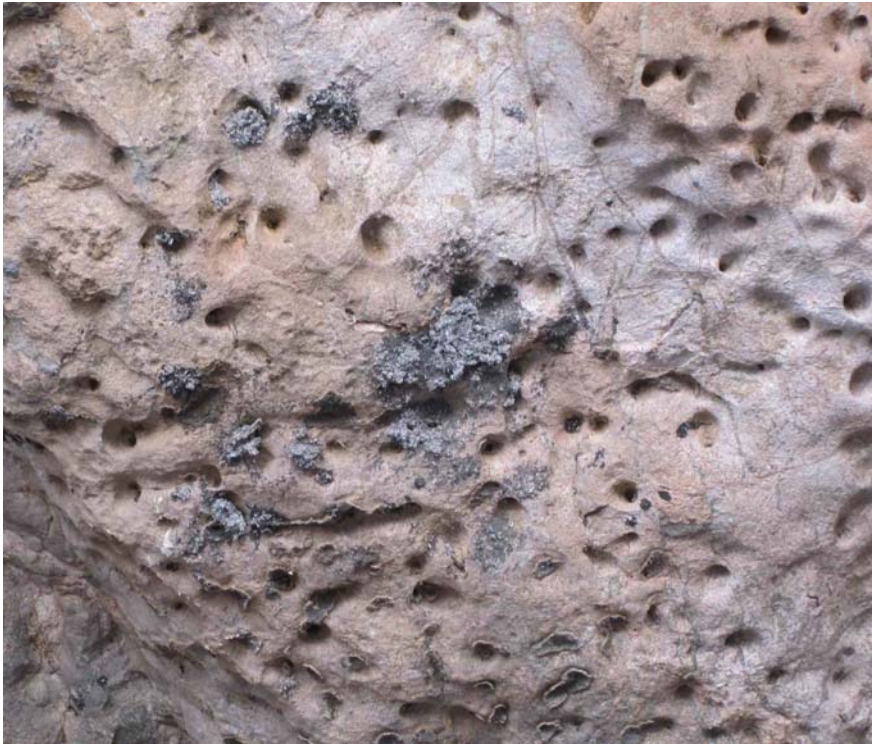


Fig. 45. Scattered remnants of the deepest portions of *Lithophaga* boreholes, bored into the roof of a marine notch during the last interglacial highstand. The conical shape is probably caused by abrasion. Holes were inaccessible to direct measurement; their inner part is ca. 2 cm diameter. James Bond Island, Phang Nga, Thailand. Photo: Kázmér #101.6991



Fig. 46. Dense network of eroded *Lithophaga* boreholes, bored into the roof of a marine notch during the last interglacial highstand. The original diameter of individual holes was about 2 cm and increased due to subsequent dissolution. Some of the boreholes coalesced to form larger

apertures. Image width ca. 1 m. James Bond Island, Phang Nga, Thailand. Photo: Kázmér #101.6990



Fig. 47. Roof of a marine notch formed during the last interglacial and thoroughly bored by *Lithophaga*. All holes have been eroded so that only their deepest parts remain in the form of circular scars. The original diameters of about 2 cm were increased by dissolution and coalescence. James Bond Island, Phang Nga, Thailand. Photo: Kázmér #101.6829



Fig. 48. Floor of a marine notch thoroughly bored by *Lithophaga*. The originally dumbbell-shaped portions of the holes – which held the animals' siphons – were all eroded, leaving behind

circular openings. Pen for scale. Near Phra Nang Cave, Railay, Krabi, Thailand. Photo: Kázmér #101.7855

Tridacna

Tridacna bivalves are important bioeroders in tropical seas. They may be seen in the intertidal zone of rocky shores, but are more common in subtidal areas where they are commonly seen drilling into live coral. They create lenticular holes to whose bottoms they are permanently attached. The elliptical openings of the holes are large enough that the shell and soft tissue are clearly visible, but may be smaller than the full size of the resident animal.



Fig. 49. **a.** Recently dead *Tridacna* in its hole; the shell has not yet been eroded. **b.** Eroded *Tridacna* borehole; impression of *Tridacna* commissure is still visible. **c.** Slightly eroded *Lithophaga* boreholes. **d.** Deeply eroded *Lithophaga* boreholes. Miocene limestone bedrock. Coin 24 mm diameter. Malakal, Palau. (Photo: Kázmér #101.9799)



Fig. 50. Dead *Tridacna* shells bored into Miocene limestone. Uniform diameter holes are deeply eroded *Lithophaga* boreholes. Coin 24 mm diameter. Malakal, Palau. (Photo: Kázmér #101.9770)

Wood-boring bivalves

It might be interesting to mention here that a significant group of bivalves specializes in mechanical boring into wood substrates. The chosen substrates are typically dead pieces of driftwood, but may also include living mangrove trees. Wood thoroughly permeated by bivalve boreholes is often found washed up on sandy beaches.



Fig. 51. Piece of driftwood heavily drilled by teredinid wood-boring bivalves. Note that the openings of borings are perpendicular to the surface, flattening at depth, being parallel to the wood grain. Scale in centimetres. Socotra, Yemen. Photo: Taboroši #DSC_9888 .

Worms

Boring worms are ubiquitous in intertidal environments; however, they are rarely recorded. The small size of the opening, often hidden by algal turf, and their superficial similarity to intact surfaces of boring sponge-infested rocks are the main problems.



Fig. 52. Wave-rounded piece of coral exhibiting small boreholes of worms, 1-2 mm in diameter. Note the paired openings! Scale in centimetres. Socotra, Yemen. Photo: Taboroši #DSC_9892 .

Sea urchins

Echinometra

Echinoids feed on algae and are capable of rasping the bedrock with their rapidly growing calcite teeth. Some genera, particularly *Echinometra*, live in the intertidal zone and are especially effective bioeroders. In addition to rasping the rock surfaces as part of the grazing process, they excavate individual hiding burrows during their lifetime. With time, burrows may extend into galleries and coalesce into overhanging ledges and wider pans.



Fig. 53. Sea urchin *Echinometra* hiding in a self-made burrow with a V-shaped cross-section in sub-vertical plane. The slopes of the burrow are surfaces which the urchin grazes regularly. Scale extended 20 cm. Okinawa. Photo: Kázmér #101.8644.



Fig. 54. Sea urchin *Echinometra* hiding in a self-made burrow whose vertical extent is V-shaped. The slopes of the burrow are surfaces which the urchin grazes regularly. Okinawa. Photo: Kázmér #101.8654.



Fig. 55. *Echinometra* burrow with a V-shaped cross-section in horizontal plane. Scale in centimetres. Okinawa. Photo: Kázmér #101.8650.



Fig. 56. *Echinometra* burrow with asymmetrical branches of a V-shaped vertical burrow. Tape measure extended 20 cm. Okinawa. Photo: Kázmér #101.8649.



Fig. 57. Variations of *Echinometra* burrows. Tape measure extended 20 cm. Okinawa. Photo: Kázmér #101.8651.



Fig. 58. Coalesced *Echinometra* burrows. Tape measure extended 20 cm. Okinawa. Photo: Kázmér #101.8648.



Fig. 59. Sea urchins *Echinometra* produced adjacent burrows in algal gardens. Burrows are arranged parallel for optimal use of available space. Tape measure extended 20 cm. Okinawa. Photo: Kázmér #101.8658



Fig. 60. Sea urchins *Echinometra* with a parallel array of adjacent algal gardens. Separating walls have been eroded away during the growth of the animals. Relief lowered about 10-15 cm during the lifetime of the animals, at a rate of approximately 1 cm/year. Okinawa. Photo: Kázmér #101.8665



Fig. 61. Winding galleries excavated by sea urchins in young basalt. Note the colourful microbial cover the echinoids feed on. Big Island, Hawai'i. Photo: Taboroši #DSC_1275 .



Fig. 62. Sea urchins in their own cavities. When these amalgamate, tidal pans will form. Tape measure extended 20 cm. Okinawa. Photo: Kázmér #101.8613.



Fig. 63. Sea urchins trying to hide under the ledge made by themselves along the perimeter of a tidal pan. Okinawa. Photo: Kázmér #101.8631



Fig. 64. Sea urchins hiding under the ledge made by themselves. Okinawa. Photo: Kázmér #101.8592



Fig. 65. Abandoned *Echinometra* burrows forming a pronounced ledge at the margin of a tidal terrace. Scale: 20 cm tape measure. Okinawa. Photo: Kázmér #101.8640



Fig. 66. Burrowing traces of young *Echinometra*. Scale: 20 cm tape measure. Okinawa. Photo: Kázmér #101.8726



Fig. 67. Tidal pans made by *Echinometra*. Okinawa. Photo: Kázmér #101.8590

Fossil echinoid burrows



Fig. 68. Fossil, eroded, uplifted sea urchin boreholes in a notch roof, about 20 cm deep. Pen 12 mm diameter. Railay, Thailand. Photo: Kázmér #102.0772



Fig. 69. Fossil sea urchin scars in the roof of an uplifted notch. Pen 12 mm diameter. Railay, Thailand. Photo: Kázmér #102.0775



Fig. 70. Fossil sea urchin scars in the roof of an uplifted notch. Only the bottoms of originally 20 cm deep boreholes are preserved. Pen 12 mm diameter. Railay, Thailand. Photo: Kázmér #102.0764.



Fig. 71. Uplifted fossil sea urchin scars perforating a fault breccia. Pen for scale. Railay, Thailand. Photo: Kázmér #102.0774



Fig. 72. Subfossil sea urchin scars perforating the seaward margin of a tidal platform in Permian limestone. Pen 12 mm diameter. Railay, Thailand. Photo: Kázmér #102.0573



Fig. 73. Uplifted sea urchin scars just above the beach. The uniform-sized boreholes were about 20 cm deep before erosion, defining acute angle with the Permian limestone wall. Pen for scale. Railay, Thailand. Photo: Kázmér #102.0790

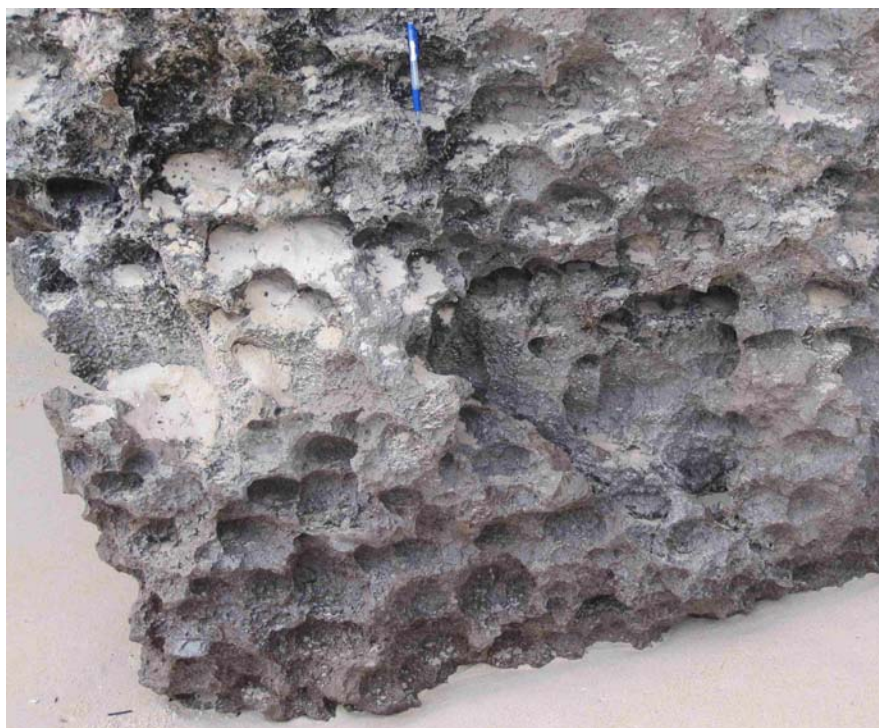


Fig. 74. Uplifted sea urchin scars observed in bedrock partly buried by beach sand. The uniform-sized boreholes were about 20 cm deep. Only their deepest parts survived coastal erosion. Permian limestone wall. Pen for scale. Railay, Thailand. Photo: Kázmér #102.0789

Crabs

Crabs are generally not considered important bioeroders, though some are known to abrade limestone surfaces in search of food. Grapsid crabs, in particular, leave visible markings in the biofilms coating supratidal areas. Though damage to the bedrock cannot be seen by the naked eye, the crabs' light-colored fecal pellets indicate high CaCO_3 content.

Grapsid crabs



Fig. 75. Fecal pellets of grapsid crabs. They are commonly observed high in the supratidal zone well beyond the reach of less motile invertebrates (such as chitons and gastropods). Light color of the pellets is indicative of high- CaCO_3 content. Guam. Photo: Taboroši #DSC_0573 .



Fig. 76. Grazing traces left by grapsid crabs feeding on dark microbial biofilm. Guam. Photo: Taboroši #DSC_1125 .

Competition and succession of bioeroders – formation of a composite landscape

Though there are many examples of rock surfaces shaped by locally dominant and particularly prolific organisms of the same or several similar species or genera, textures on coastal bedrock are more often compound results of bioerosional activities of a variety of contemporary (and competing) or successive taxa. Here we examine several examples of small-scale composite landscapes created by heterogeneous organisms operating in the same locations, though not necessarily at the same time.

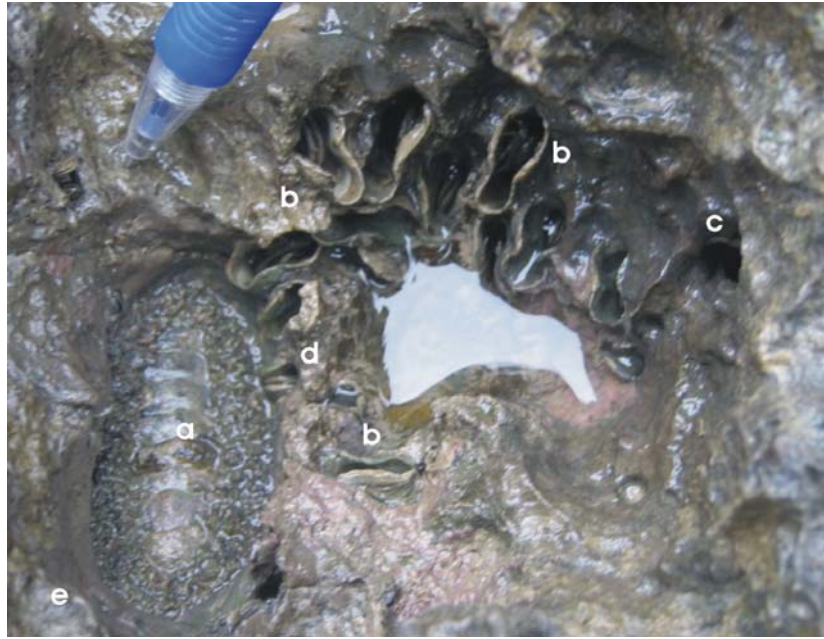


Fig. 77. Chiton grazing traces and *Lithophaga* borings as a result of competition for space. **a.** Chiton in the homing scar. **b.** Current-generation, living *Lithophaga* in borehole. Light-coloured, calcareous lining of borehole emergent above rock surface. **c.** Past-generation *Lithophaga* borehole, eroded halfway down. **d.** Current-generation *Lithophaga* borehole whose calcareous lining is lacking, possibly having been breached by expansion of the chiton's homing scar. Double valves of the bivalve are visible in the borehole. Overall surface lowering is mostly due to chiton grazing. Pen for scale. Railay, Thailand. Photo: Kázmér #102.0906



Fig. 78. Traces of a boring sponge colony. Small holes at lower left are original openings. Larger holes in the middle are interconnected sponge chambers whose roofs have been eroded. Two damaged, angular *Lithophaga* borings in the upper right are older than sponge infestation and their walls also contain sponge chamber openings. Two round *Lithophaga* boreholes in the top centre of the image are younger than sponge activity and lack evidence of sponge chambers in their walls. Coin 24 mm diameter. Palau. Photo: Kázmér #101.9773.



Fig. 79. Traces of a boring sponge colony. Interconnected chamber system is exposed beneath eroded surface. There are some heavily damaged *Lithophaga* boreholes in the lower left corner. Pen 12 mm diameter. Palau. Photo: Kázmér #101.8552.



Fig. 80. *Lithophaga* burrows and dead shells in place, partially eroded and exposed by chiton grazing. Coin 20 mm diameter. Naha, Okinawa. Photo: Kázmér #101.8437



Fig. 81. Boulder heavily bored by *Lithophaga*. First generation of bioeroders are sponges (top of image), second generation *Lithophaga*. All of their holes are devoid of sponge borings. A third generation bioeroder (or physical erosion) removed the top of the *Lithophaga* borings, exposing the circular portion of the holes. Istria, Croatia. Photo: Taboroši #DSC_6475.

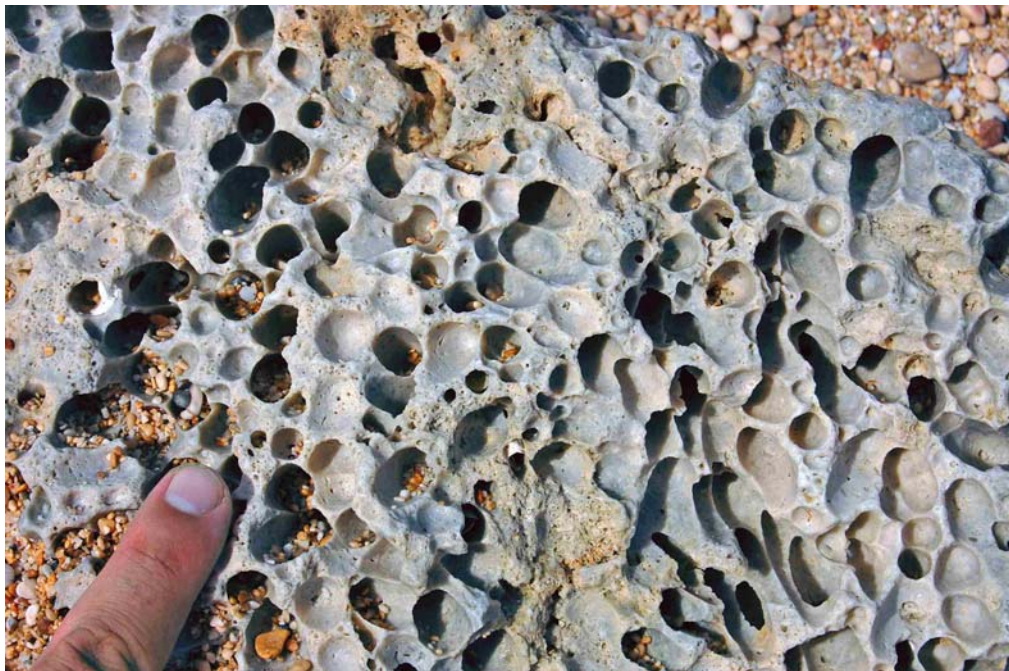


Fig. 82. A first generation of sponge-infested surface (see remnants of chambers on ridges only) were bored by *Lithophaga*. Subsequently the surface layer of the rock was removed and the circular portion of the boreholes exposed. Most of the bored rock has been removed by erosion. Only innermost ends of boreholes are still visible. Lack of sponge chambers within the *Lithophaga* borings proves the succession. Ras al Jinz, Oman. Photo: Taboroši #DSC_9367.



Fig. 83. Hand specimen of a limestone rock heavily drilled a first generation of boring sponges and by a second generation of *Lithophaga* bivalves. The second generation has intact shells within the holes, protruding above hole margins. The third generation of bioeroders exposing the *Lithophaga* boreholes is unknown (chiton?). Kraljevica, Croatia. Photo: Taboroši #DSC_9870.



Fig. 84. Dynamic landscape created by bioerosion. Chiton and *Lithophaga* borings and encrusting oyster shells compete for space. **a.** Chiton grazing traces. **b.** Older generation of eroded *Lithophaga* boreholes with about half of their original depth missing. **c.** Dumbbell-shaped openings of younger generation of *Lithophaga* burrows. **d.** Dead oyster shell, intact by erosion. **e.** Largely eroded oyster shell. **f.** Chiton responsible for grazing erosion at this location. Pen 12 mm diameter. Railay, Thailand. Photo: Kázmér #102.0903

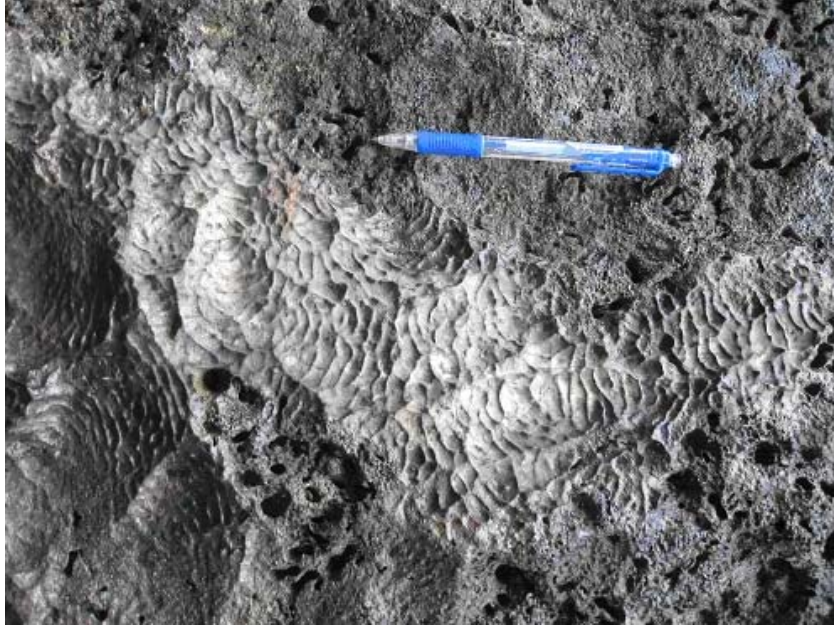


Fig. 85. Chiton grazing and *Lithophaga* borings compete for space. Note the lack of grazing marks in the immediate vicinity of borehole openings, indicating that the chiton avoided that area. Railay, Thailand. Photo: Kázmér #102.0595

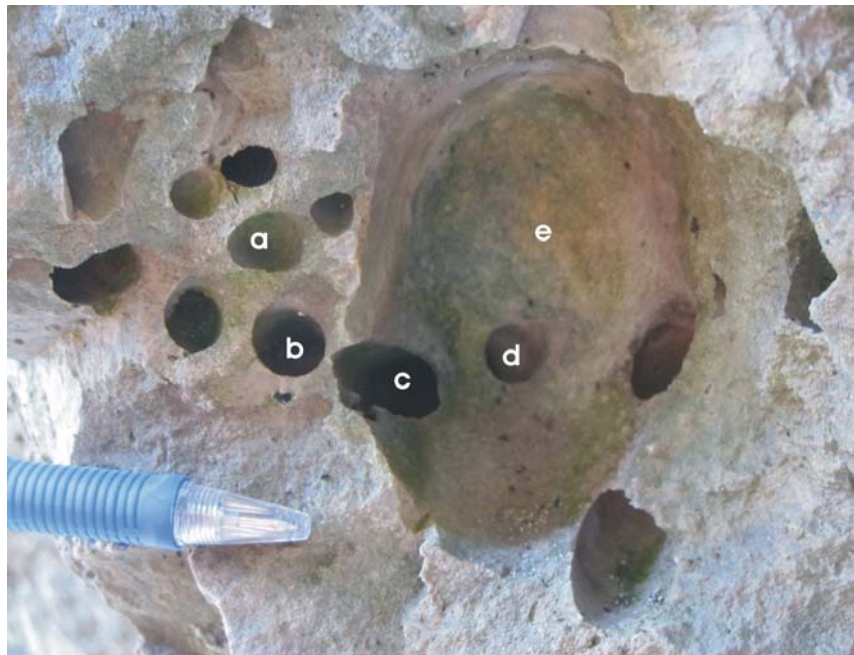


Fig. 86. Chiton grazing traces and *Lithophaga* borings compete for space. **a.** First generation of *Lithophaga* borehole, almost completely eroded. **b.** Second generation of *Lithophaga* borehole, penetrating deeper than the first generation (due to erosion of the surface in the meantime); only the upper half is eroded. **c.** *Lithophaga* burrow of the second generation, eroded laterally by chiton making the homing scar. **d.** *Lithophaga* burrow of the second generation, eroded to the bottom. **e.** Bottom of a chiton homing scar: this is the third generation of boring at this location. Surface lowering is mostly due to chiton grazing. Pen 12 mm diameter. Koh Hong, Krabi, Thailand. Photo: Kázmér #101.7529



Fig. 87. Chiton hiding in homing scar. Littorinid gastropods aggregate during low tide. Eroded *Lithophaga* burrow in lower right corner. Coin 24 mm diameter. Palau. Photo: Kázmér #101.9792



Fig. 88. A variety of smaller bioeroders: worms and/or boring sponges. Pen for scale. Okinawa. Photo: Kázmér #101.8496



Fig. 89. A landscape devastated by a succession of bioeroders, with the chiton hiding in the right-hand side of the image being the most recent culprit. Pen 12 mm diameter. Okinawa. Photo: Kázmér 101.8505.

Pseudo-bioerosion

Here we provide several useful examples of phenomena that are somewhat similar to and may be confused with bioerosional features, particularly by inexperienced students beginning work in an unfamiliar field area.



Fig. 90. Coral colony embedded in the Pleistocene Ryukyu Limestone, exposed by erosion of the fine-grained matrix. The circular hole enclosing the coral is a reflection of the coral's rounded shape. Not a sediment-filled echinoid burrow. Pen for scale. Okinawa. Photo: Kázmér #101.8530



Fig. 91. Hole remaining after a chert nodule has fallen off from the notch wall. Not an eroded echinoid burrow. Pen 12 mm diameter. Railay, Thailand. Photo: Kázmér: #102.0561.



Fig. 92. Chert nodules in coastal micrite. **a.** an intact nodule. **b.** partially broken nodule. **c.** hole left behind by a nodule that has fallen out. Lebanon. Photo: Taboroši #DSC_2833 .



Fig. 93. Chert nodules weather faster than the host limestone in the intertidal zone under wave action and leave behind holes of various shapes. Not sediment-filled echinoid burrows. Railay, Thailand. Photo: Kázmér #102.0564



Fig. 94. Dissolutionally etched rock surface in the spray zone of an uplifted notch roof, grazed by *Littorina*. Pen for scale. Railay, Thailand. Photo: Kázmér #102.0596

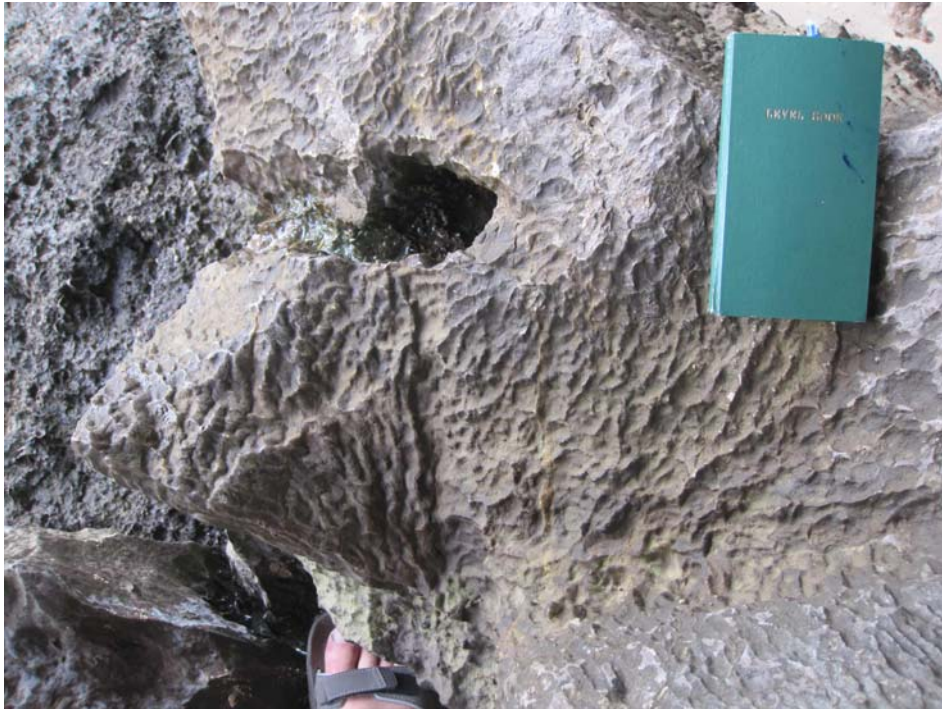


Fig. 95. Vertical karren ridges formed on the rock surface of a collapsed boulder. Field notebook 16.5 cm long. Railay, Thailand. Photo: Kázmér #102.0783

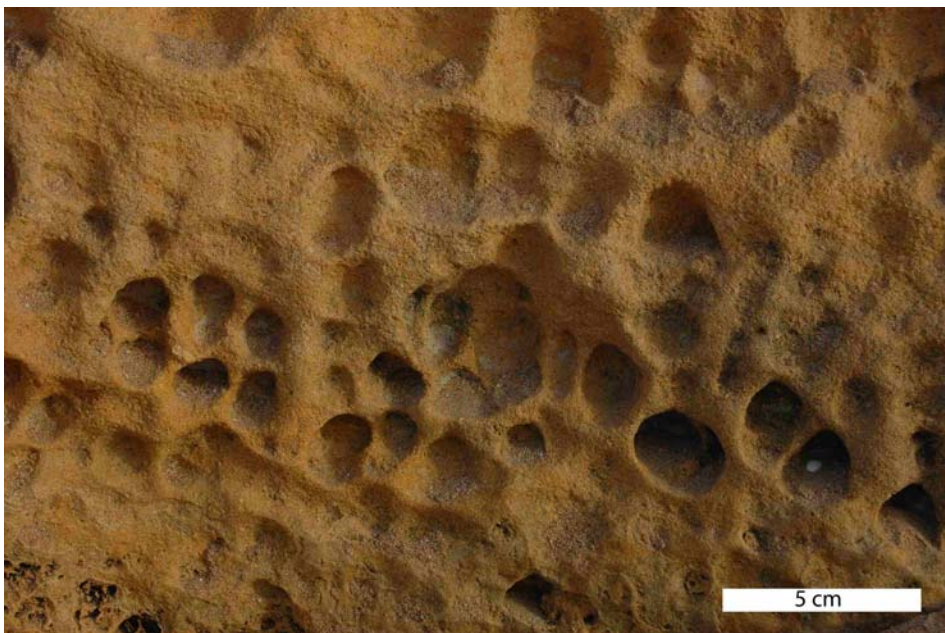


Fig. 96. Tafoni weathering in coastal sandstone. Not termini of *Lithophaga* boreholes. Ras al Jinz, Oman. Photo: Taboroši #DSC_9087.

Acknowledgements

The authors are grateful to Pat and Lori COLIN (Coral Reef Research Foundation, Koror, Palau), Frank OHLINGER (Koror, Palau), Akira MAEKADO and Ryuji ASAMI (both at the University of the Ryukyus, Okinawa), Kenjiro SHO (Nagoya University of Technology), Yasufumi IRYU (Nagoya University), Oki SUGIMOTO (JICA, Tokyo), Gábor KONDOROSI (Tokyo), Punya CHARUSIRI and Santi PAILOPLEE (both at Chulalongkorn University, Bangkok, Thailand), Fami YUSOH (Penang, Malaysia), Wikrom BUAPAN (Krabi, Thailand) for their hospitality, kind advices, and help in the field. Sincere thanks are due to Bosiljka GLUMAC (Smith College, Northampton, Massachusetts, USA) for Figs. 26 and 31; to Matthieu SONTAG for Fig. 6 (Licence CC-BY-SA). Large portion of the results presented in this paper were obtained during fieldwork for a study supported by Hungarian National Science Foundation, OTKA grant K 67,583. The European Union and the European Social Fund have provided financial support M.K. during the project under the grant agreement no. TÁMOP 4.2.1./B-09/1/KMR-2010-0003.

References

- GLAUB, I., GOLUBIC, S., GEKTIDIS, M., RADTKE, G. AND VOGEL, K. (2007) Microborings and microbial endoliths: Geological implications. In: MILLER, W. C. (ed.) Trace fossils: concepts, problems, prospects, Elsevier, 368-381.
- EKDALE, A.A., BROMLEY, R.G. & PEMBERTON, S.G. 1984. Ichnology: The use of trace fossils in sedimentology and stratigraphy: SEPM Publication, Tulsa, OK.
- JONES, B. (1989) The role of microorganisms in phytokarst development on dolostones and limestones, Grand Cayman, British West Indies. Canadian Journal of Earth Sciences 26, 2204–2213.
- RASMUSSEN, K.A. & FRANKENBERG, E.W. 1990. Intertidal bioerosion by the chiton *Acanthopleura granulata*: San Salvador, Bahamas. – Bulletin of Marine Science 47/3, 680-695.
- SPENCER, T. & VILES, H. 2002. Bioconstruction, bioerosion and disturbance on tropical coasts: Coral reefs and rocky limestone shores. Geomorphology, 48:23–50.

Table 1. Geographical coordinates of locations (where available).

Figure nr.	Photo #	Country	Island / Prov.	Coast	Latitude	Longitude
1	101.9767	Palau	Malakal	dam	N 7° 20' 27,3"	E 134° 27' 44.3"
10	101.9791.	Palau	Malakal	dam	N 7° 20' 27,3"	E 134° 27' 44.3"
11	101.8491	Japan	Okinawa	Cape Ara	N 26° 4' 44"	E 127° 40' 9.4"
12	101.8732	Japan	Okinawa	Cape Hedo	N 26° 52' 2.2"	E 128° 15' 41,6"
13	101.9780	Palau	Malakal	dam	N 7° 20' 27,3"	E 134° 27' 44.3"
14	101.9789	Palau	Malakal	dam	N 7° 20' 27,3"	E 134° 27' 44.3"
15	101.9796	Palau	Malakal	dam	N 7° 20' 27,3"	E 134° 27' 44.3"
16	102.0602	Thailand	Krabi	Railay	N 8° 1' 6.2"	E 98° 51' 6.7"
17	102.0777	Thailand	Krabi	Railay, Phra Nang	N 8° 0' 14.9"	E 98° 50' 24.6"
18	102.0778	Thailand	Krabi	Railay, Phra Nang	N 8° 0' 14.9"	E 98° 50' 24.6"
19	102.0901	Thailand	Krabi	Railay	N 8° 0' 25.9"	E 98° 50' 32"
20	101.8711	Japan	Okinawa	Cape Hedo	N 26° 52' 2.2"	E 128° 15' 41,6"
21	102.0592	Thailand	Krabi	Railay	N 8° 1' 6.2"	E 98° 51' 6.7"
22	101.9797	Palau	Malakal	dam	N 7° 20' 27,3"	E 134° 27' 44.3"
23	101.9787	Palau	Malakal	dam	N 7° 20' 27,3"	E 134° 27' 44.3"

Figure nr.	Photo #	Country	Island / Prov.	Coast	Latitude	Longitude
24	102.0891	Thailand	Krabi	Railay	N 8° 0' 25.9"	E 98° 50' 32"
25	101.8730	Japan	Okinawa	Cape Hedo	N 26° 52' 2.2"	E 128° 15' 41.6"
30	101.8273	Japan	Okinawa	Naha, Naminoue	N 26° 13' 15.8"	E 127° 40' 17.0"
34	102.0582	Thailand	Krabi	Railay	N 8° 1' 6.2"	E 98° 51' 6.7"
36	101.0881	Thailand	Krabi	Railay	N 8° 0' 25.9"	E 98° 50' 32"
37	101.8440	Japan	Okinawa	Miibaru	N 26° 7' 58.5"	E 127° 47' 17.7"
38	101.0882	Thailand	Krabi	Railay	N 8° 0' 25.9"	E 98° 50' 32"
39	102.0570	Thailand	Krabi	Railay	N 8° 1' 6.2"	E 98° 51' 6.7"
40	102.0589	Thailand	Krabi	Railay	N 8° 0' 57.7"	E 98° 51' 1.4"
41	102.0811	Thailand	Krabi	Railay	N 8° 0' 14.9"	E 98° 50' 24.6"
42	102.0547	Thailand	Krabi	Railay	N 8° 0' 47"	E 98° 50' 53.6"
43	102.0571	Thailand	Krabi	Railay	N 8° 1' 6.2"	E 98° 51' 6.7"
44	101.6817	Thailand	Phang Nga	James Bond Island	N 8° 16' 28"	E 98° 30' 3.4"
45	101.6991	Thailand	Phang Nga	James Bond Island	N 8° 16' 26.6"	E 98° 29' 59"
46	101.6990	Thailand	Phang Nga	James Bond Island	N 8° 16' 26.6"	E 98° 29' 59"
47	101.6829	Thailand	Phang Nga	James Bond Island	N 8° 16' 28"	E 98° 30' 3.4"
48	101.7855	Thailand	Krabi	Railay, Phra Nang	N 8° 0' 14.9"	E 98° 50' 24.6"
49	101.9799	Palau	Malakal	dam	N 7° 20' 27.3"	E 134° 27' 44.3"
50	101.9770	Palau	Malakal	dam	N 7° 20' 27.3"	E 134° 27' 44.3"
53	101.8644	Japan	Okinawa	Koure	N 26° 42' 48.3"	E 128° 1' 7.3"
54	101.8654	Japan	Okinawa	Koure	N 26° 42' 48.9"	E 128° 1' 7.3"
55	101.8650	Japan	Okinawa	Koure	N 26° 42' 48.9"	E 128° 1' 7.3"
56	101.8549	Japan	Okinawa	Koure	N 26° 42' 48.9"	E 128° 1' 7.3"
57	101.8651	Japan	Okinawa	Koure	N 26° 42' 48.9"	E 128° 1' 7.3"
58	101.8648	Japan	Okinawa	Koure	N 26° 42' 48.9"	E 128° 1' 7.3"
59	101.8658	Japan	Okinawa	Koure	N 26° 42' 48.3"	E 128° 1' 7.3"
60	101.8665	Japan	Okinawa	Koure	N 26° 42' 48.3"	E 128° 1' 7.3"
62	101.8613	Japan	Kume	Koure	N 26° 41' 59.5"	E 128° 1' 37.2"
63	101.8631	Japan	Okinawa	Koure	N 26° 42' 48.9"	E 128° 1' 7.3"
64	101.8592	Japan	Kume	Koure	N 26° 41' 59.5"	E 128° 1' 37.2"
65	101.8640	Japan	Okinawa	Koure	N 26° 42' 48.9"	E 128° 1' 7.3"
66	101.8726	Japan	Okinawa	Koure	N 26° 42' 48.9"	E 128° 1' 7.3"
67	101.8590	Japan	Okinawa	Koure	N 26° 41' 59.5"	E 128° 1' 37.2"
68	102.0772	Thailand	Krabi	Railay, Phra Nang	N 8° 0' 14.9"	E 98° 50' 24.6"
69	102.0775	Thailand	Krabi	Railay, Phra Nang	N 8° 0' 14.9"	E 98° 50' 24.6"
70	102.0764	Thailand	Krabi	Railay, Phra Nang	N 8° 0' 14.9"	E 98° 50' 24.6"
71	102.0774	Thailand	Krabi	Railay, Phra Nang	N 8° 0' 14.9"	E 98° 50' 24.6"
72	102.0573	Thailand	Krabi	Railay	N 8° 0' 57.7"	E 98° 51' 1.4"
73	102.0790	Thailand	Krabi	Railay, Phra Nang	N 8° 0' 14.9"	E 98° 50' 24.6"
74	102.0789	Thailand	Krabi	Railay, Phra Nang	N 8° 0' 14.9"	E 98° 50' 24.6"
77	102.0906	Thailand	Krabi	Railay	N 8° 0' 25.9"	E 98° 50' 32"
78	101.9773	Palau	Malakal	dam	N 7° 20' 27.3"	E 134° 27' 44.3"
79	101.8552	Japan	Okinawa	Miyagi, Hamahiga	N 26° 19' 39.6"	E 127° 57' 29.8"
80	101.8437	Japan	Okinawa	Miibaru	N 26° 7' 58.5"	E 127° 47' 17.7"
84	102.0903	Thailand	Krabi	Railay	N 8° 0' 25.9"	E 98° 50' 32"
85	102.0595	Thailand	Krabi	Railay	N 8° 01' 6.2"	E 98° 51' 6.7"
86	101.7529	Thailand	Krabi	Koh Hong	N 8° 4' 45.3"	E 98° 40' 52.8"
87	101.9792	Palau	Malakal	dam	N 7° 20' 27.3"	E 134° 27' 44.3"
88	101.8496	Japan	Okinawa	Cape Ara	N 26° 4' 44"	E 127° 40' 9.4"
89	101.8505	Japan	Okinawa	Cape Ara	N 26° 4' 44"	E 127° 40' 9.4"

Figure nr.	Photo #	Country	Island / Prov.	Coast	Latitude	Longitude
90	101.8530	Japan	Okinawa	Cape Ara	N 26° 4' 56.0"	E 127° 41' 16.3"
91	102.0561	Thailand	Krabi	Railay	N 8° 0' 59.7"	E 98° 51' 1.4"
93	102.0564	Thailand	Krabi	Railay	N 8° 0' 59.7"	E 98° 51' 1.4"
94	102.0596	Thailand	Krabi	Railay	N 8° 1' 6.2"	E 98° 51' 6.7"
95	102.0783	Thailand	Krabi	Railay, Phra Nang	N 8° 0' 14.9"	E 98° 50' 24.6"